

Update: A new method for three-dimensional visualization and quantification of biogenic structures in aquatic sediments using axial tomodensitometry

Suzanne C. Dufour¹, Gaston Desrosiers¹, Bernard Long², Patrick Lajeunesse³, Marie Gagnoud¹, Jacques Labrie², Philippe Archambault⁴, and Georges Stora⁵

¹Institut des Sciences de la Mer de Rimouski, Université du Québec à Rimouski, 310 allée des Ursulines, Rimouski (Québec) G5L 3A1 Canada

²Institut National de la Recherche Scientifique, INRS-ETE, 490 de la Couronne, Québec (Québec) G1K 9A9 Canada

³Centre d'Études Nordiques, Université Laval, Québec (Québec) G1K 7P4 Canada

⁴Institut Maurice-Lamontagne, Environmental Science Division, 850 Route de la Mer, P.O. Box 1000, Mont-Joli (Québec) G5H 3Z4 Canada

⁵Laboratoire de Microbiologie Géochimie et Écologie Marines, Centre d'Océanologie de Marseille, Université de la Méditerranée, Campus de Luminy – Case 901, 163 Avenue de Luminy, 13288 Marseille Cedex 9 France

The technique described by Dufour et al. (2005) was found to be inaccurate in some instances due to problems associated with the estimation of the theoretical sediment curve. For example, in sediment sections containing more than 10% dense material (e.g., rocks, shells), the TSC often had a larger spread than that of the sediment, and the resulting percentage of biogenic structure and organic matter occupation was underestimated (Fig. 1A). In other cases, the curve representing sediments was bimodal, and the mean of the TSC was placed at the larger peak; if this peak happened to be on the right, then the percent of occupation was overestimated (Fig. 1B). Attempts to manually fix these problems were largely unsatisfactory and time consuming, thereby defeating the purpose of an automated algorithm. Problems with the TSC also led to large variability and likely overestimates of percent organic matter + air-filled structures (fig. 3 of Dufour et al. 2005).

An alternate approach to estimating the TSC is based on the premise that each scanned section of a sediment core contains a certain number of materials, each of which has an approximately Gaussian distribution of TI values. Symmetrical Gaussian curves are fitted to the data, and the proportion of area underneath the curves corresponding to water, organic matter, and air (if present) estimates the proportion of biogenic space occupation in the given section.

The CT-data obtained for the three cores presented in Dufour et al. (2005, fig. 2 and fig. 3) are re-analyzed using the new approach. The Gaussian fits are calculated iteratively using an Expectation Maximization (EM) algorithm (modified from code by O. Gal, function #3, <http://www.mathworks.com/matlabcentral/fileexchange/loadFile.do?objectId=4222&objectType=FILE>) in the software Matlab 6.0 (Mathworks, Natick, MA). In the program used, the number of Gaussian curves must be preselected. We chose to fit three curves on all TI values between -224 and 1076 HU that should include TI “populations” of water, organic matter, and sediment. Pixels having TI values <-224 HU (air-filled voids) and >1076 HU (dense sediments, rocks, and carbonates) are excluded to speed the analysis (more Gaussian curves requires a longer iteration). The threshold TI values were determined after careful observation of a substantial number of graphs of pixel number versus TI value, as well as CT images of the corresponding sections.

From three starting points equally distributed along the x-axis, the Gaussian curves converge iteratively toward local maxima that become the Gaussian means. The sum of the fitted Gaussian curves closely approximates the data (Fig. 2). In cases where it is only possible to fit two Gaussian curves to the data (Fig. 2B), the first curve is set to the extreme left of the x-axis and ignored from the analysis.

To calculate biogenic occupation in a given section, it is first necessary to examine the fitted Gaussian curves to determine which one(s) represent(s) water and/or organic matter; either one of the leftmost curves (G1 or G2) or both of them (G1 + G2). The rightmost curve (i.e., higher TI values) corresponds to sediments. Knowing that $G_1+G_2+G_3 = 1$ and G_i represents the area beneath the i th curve, and also knowing the

*Corresponding author's e-mail: suzanne.dufour@gmail.com

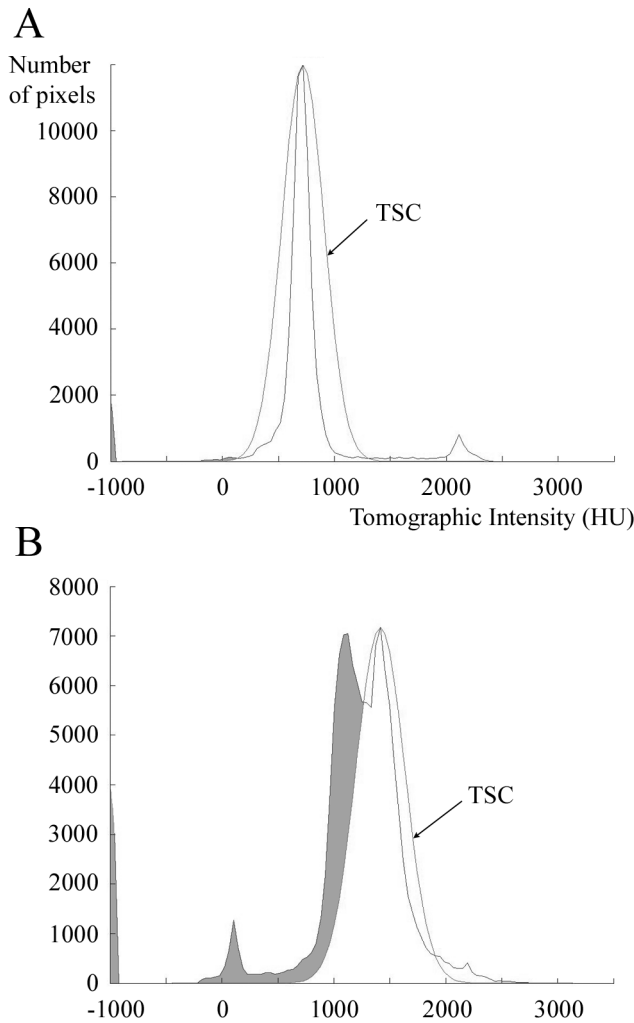


Fig. 1. Examples of automated total sediment curve (TSC) determinations that led to erroneous results. Graphs show the number of pixels versus tomographic intensity for a 1 mm CT slice of a sediment core, along with the TSC and, in gray, the values to the left of the TSC representing space occupied by organic matter and air/water-filled structures in the sediment (S). A. Due to the peak of high-density material such as rocks at about 2000 HU, the standard deviation of the TSC is too large, and S is underestimated. B. Due to the bimodal peak in sediments, S is overestimated.

total number of pixels in the analyzed section (N), the number of pixels for $TI < -224$ HU ($N_{<-224}$) and for $-224 < TI < 1076$ HU ($N_{-224-1076}$), as well as the values for G1 and G2, then spatial occupation [S] is:

$$S = \frac{(G_1 N_{-224-1076}) + N_{<-224}}{N} \times 100 \quad (1)$$

where G_i is either G1, G2, or the sum of G1 and G2.

Re-analysis of the cores represented in fig. 2 and fig. 3 of Dufour et al. (2005) using the Gaussian fitting technique resulted in depth profiles of spatial occupation that differed from those obtained previously (Fig. 3). In particular, the

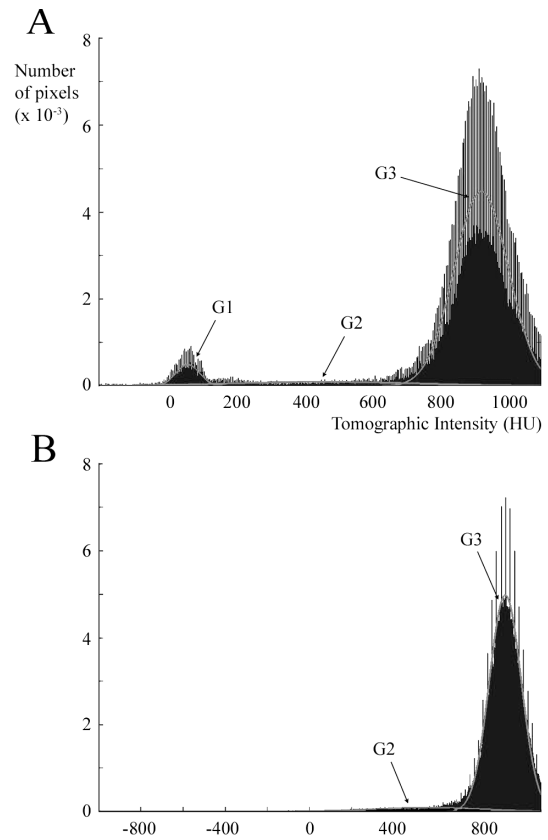


Fig. 2. Fitting of Gaussian curves (in gray) to number of pixels versus tomographic intensity data for two 1 mm CT slices. A. Three Gaussian curves, corresponding to water (G1), organic matter/interfaces (G2), and sediments (G3). B. In this section, only two Gaussian curves (G2 and G3) are fitted; G1 is positioned at the extreme left of the x axis and has a standard deviation of 1.

curves have a smaller and probably more accurate range of values compared to the original curves. Spatial occupation appears more constant in the cores from St-Siméon and Barachois (Fig. 3B, Fig. 3C) using the new technique. This result would seem to better correspond to the CT-images of these cores (fig. 2B, fig. 2C, Dufour et al. 2005), where spatial occupation with depth seems more likely to vary by a few percent than by over 70%.

Compared with the threshold technique (e.g., de Montey et al., 2003; Mermillod-Blondin et al. 2003; Michaud et al. 2003), the Gaussian fitting algorithm yields similar spatial occupation values (Fig. 4). In contrast, the TSC method of Dufour et al. (2005) either overestimates or underestimates spatial occupation values, especially in parts of the core with finer sediments (i.e., the clay fraction, 5–10 cm depth), or with more carbonates (i.e., the fraction containing fossilized shells, 12–16 cm depth). Thus, the Gaussian fitting technique appears to provide reliable results without the significant time investment of the threshold technique.

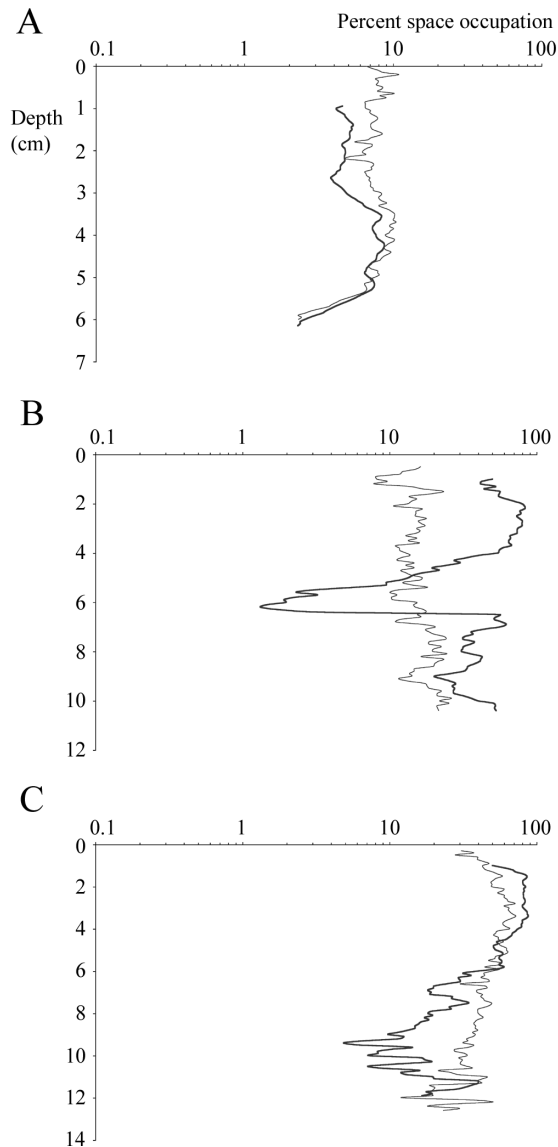


Fig. 3. Comparison of spatial occupation (air + water-filled structures + organic matter + interfaces) with depth curves using the previous technique by Dufour et al. 2005 (thick lines) and the Gaussian fitting technique (thin lines), on cores from A. Baie du Ha! Ha!, B. St-Siméon, and C. Barchois.

The new approach to calculating the space occupied by organisms and their burrows in sediment is slightly more time consuming than the automated TSC technique (~ 1 h per 10 cm core on a dual-processor running at 2.6 GHz); however, it seems comparatively more robust in accounting for the various mixtures of materials that are found in sediment cores, and provides results that appear to be more realistic.

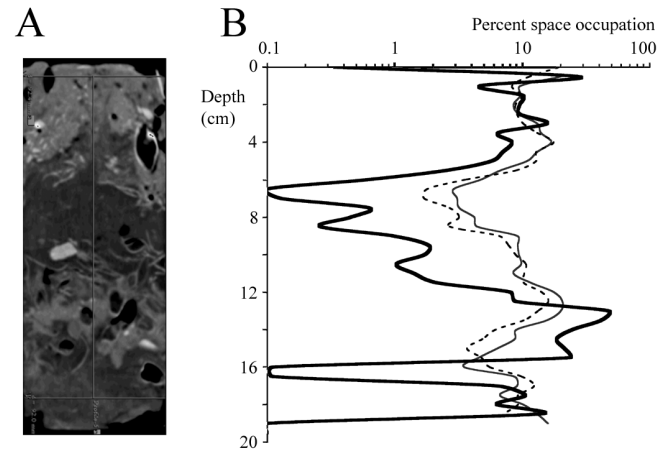


Fig. 4. Comparison of three spatial occupation techniques on a 20 cm long core from Baie du Ha! Ha!. A. Longitudinal topogram of the core, revealing muddy sand inhabited by bivalves from 0–5 cm depth, a clay facies at 5–10 cm depth, and a muddy-sand facies with shells below 10 cm depth. B. Spatial occupation determined using the manual threshold technique of de Montety et al. 2003 and Mermillod-Blondin et al. 2003 (dotted line); the previous technique by Dufour et al. 2005 (thick line) and the Gaussian fitting technique (thin line).

References

- de Montety, L., B. Long, G. Desrosiers, J.-F. Crémer, J. Locat, and G. Stora. 2003. Utilisation de la scanographie pour l'étude des sédiments: influence des paramètres physiques, chimiques et biologiques sur la mesure des intensités tomographiques. *Can. J. Earth Sci.* 40:937–948.
- Dufour, S. C., G. Desrosiers, B. Long, P. Lajeunesse, M. Gagnoud, J. Labrie, P. Archambault, and G. Stora. 2005. A new method for three-dimensional visualization and quantification of biogenic structures in aquatic sediments using axial tomodensitometry. *Limnol. Oceanogr. Meth.* 3:372–380.
- Gagnoud, M., P. Lajeunesse, G. Desrosiers, B. Long, J. Labrie, F. Mermillod-Blondin, and G. Stora. 2004. Sedimentary facies analysis of glaciomarine mud using axial tomodensitometry (CAT-scan), p. 447. *In* 32nd International Geological Congress, August 2004, Florence, Italy. International Union of Geological Sciences.
- Mermillod-Blondin, F., S. Marie, G. Desrosiers, B. Long, L. de Montety, E. Michaud, and G. Stora. 2003. Assessment of the spatial variability of intertidal benthic communities by axial tomodensitometry: importance of fine-scale heterogeneity. *J. Exp. Mar. Biol. Ecol.* 287:193–208.
- Michaud, E., and others. 2003. Use of axial tomography to follow temporal changes of benthic communities in an unstable sedimentary environment (Baie des Ha! Ha!, Saguenay Fjord). *J. Exp. Mar. Biol. Ecol.* 285–286:265–282.